YALE
PEABODY
MUSEUM

JOURNAL OF MARINE RESEARCH

The *Journal of Marine Research,* one of the oldest journals in American marine science, published important peer-reviewed original research on a broad array of topics in physical, biological, and chemical oceanography vital to the academic oceanographic community in the long and rich tradition of the Sears Foundation for Marine Research at Yale University.

An archive of all issues from 1937 to 2021 (Volume 1–79) are available through EliScholar, a digital platform for scholarly publishing provided by Yale University Library at https://elischolar.library.yale.edu/.

Requests for permission to clear rights for use of this content should be directed to the authors, their estates, or other representatives. The *Journal of Marine Research* has no contact information beyond the affiliations listed in the published articles. We ask that you provide attribution to the *Journal of Marine Research.*

Yale University provides access to these materials for educational and research purposes only. Copyright or other proprietary rights to content contained in this document may be held by individuals or entities other than, or in addition to, Yale University. You are solely responsible for determining the ownership of the copyright, and for obtaining permission for your intended use. Yale University makes no warranty that your distribution, reproduction, or other use of these materials will not infringe the rights of third parties.

Sedimentation of phytoplankton during a diatom bloom: Rates and mechanisms

by Thomas Kiørboe[1], Jørgen L. S. Hansen[2], Alice L. Alldredge[3], George A. Jackson[4], Uta Passow[3], Hans G. Dam[5], David T. Drapeau[5], Anya Waite[6,7] and Carlos M. Garcia[8]

ABSTRACT

Phytoplankton blooms are uncoupled from grazing and are normally terminated by sedimentation. There are several potential mechanisms by which phytoplankton cells may settle out of the photic zone: sinking of individual cells or chains, coagulation of cells into aggregates with high settling velocities, settling of cells attached to marine snow aggregates formed from discarded larvacean houses or pteropod feeding webs, and packaging of cells into rapidly falling zooplankton fecal pellets. We quantified the relative significance of these different mechanisms during a diatom bloom in a temperate fjord, and evaluated their potential to control phytoplankton population dynamics. Overall specific sedimentation rates of intact phytoplankton cells were low during the 11-day study period, averaging ca. 0.1 d^{-1}, and mass sedimentation and bloom termination did not occur. Most cells settled attached to marine snow aggregates formed from discarded larvacean houses, whereas settling of unaggregated cells was insignificant. Formation rates of phytoplankton aggregates by physical coagulation was very low, and losses by this mechanism were ≪0.07 d^{-1}; phytoplankton aggregates were neither recorded in the water column (by divers) nor in sediment traps. The low coagulation rates were due to a very low 'stickiness' of suspended particles. The dominant diatom, *Thalassiosira mendiolana,* that accounted for up to 75% of the phytoplankton biomass, was not sticky at all, and did not turn sticky upon nutrient depletion in culture experiments. The low particle stickiness recorded may be related to low formation rates by diatoms of transparent exopolymeric particles (TEP), that occurred in low concentrations throughout the study period. Zooplankton grazing rate did not respond to the development of the bloom and accounted for a loss term to the phytoplankton populations comparable to sinking of intact cells; fecal pellets accounted for 30–50% of settled phytoplankton and phytodetritus. While coagulation may give rise to density-dependent losses to phytoplankton populations and, hence, control blooms, neither of the other mechanisms

1. Danish Institute for Fisheries Research, Charlottenlund Castle, DK-2920 Charlottenlund, Denmark (email: tk@dfu.min.dk)
2. Marine Biological Laboratory, Strandpromenaden 5, DK-3000 Helsingør, Denmark.
3. Marine Sciences Institute, University of California, Santa Barbara, California, 93106, U.S.A.
4. Department of Oceanography, Texas A&M University, College Station, Texas, 77843, U.S.A.
5. Department of Marine Sciences, University of Connecticut, Groton, Connecticut, 06340-6097, U.S.A.
6. Woods Hole Oceanographic Institution, Woods Hole, Massachusetts, 02143, U.S.A.
7. Present address: School of Biological Sciences, Victoria University of Wellington, P.O. Box 600, Wellington, New Zealand.
8. Universidad de Cadiz, Department de Biologia Animal, Vegetal y Ecologia, Aptdo 40, E-11510 Puerto Real (Cadiz), Spain.

examined worked in a density dependent manner. In the absence of significant coagulation rates, rapid mass sedimentation of this bloom did not occur.

1. Introduction

Diatoms have population growth rates that typically exceed those of their mesozooplankton grazers by an order of magnitude or more. Such phytoplankton populations may, therefore, escape herbivore control when light and nutrients are plentiful and develop into massive blooms, especially during spring in some temperate seas. Since blooms develop exactly because grazing is uncoupled from phytoplankton growth, their fate is usually sedimentation to the sea floor rather than consumption in the water column (e.g. Legendre, 1990; Kiørboe, 1993).

There are several potential mechanisms by which diatom blooms may sediment to the sea floor. First, phytoplankton cells or chains may settle individually. Increased settling velocities of individual cells or chains due to buoyancy control or spore formation may help explain the often massive phytoplankton sedimentation on bloom termination (Bienfang, 1981a; Pitcher, 1986; Waite *et al.*, 1992a,b). However, phytoplankton settling velocities during blooms frequently exceed those of single cells or chains by an order of magnitude (e.g. Bodungen *et al.*, 1981; Passow, 1991) because live, intact cells may sediment via mm- to cm-sized aggregates with high settling velocities (Beers *et al.*, 1986; Alldredge and Silver, 1988). Rapidly settling phytoplankton aggregates have been observed repeatedly in the ocean (Kranck and Milligan, 1988; Alldredge and Gotschalk, 1989; Olesen, 1993). Coagulation of diatoms to form such aggregates has, therefore, been invoked as a second mechanism leading to the sedimentation of blooms (Jackson, 1990). Diatom aggregation by physical coagulation has been demonstrated in laboratory (Kiørboe *et al.*, 1990; Kiørboe and Hansen, 1993; Drapeau *et al.*, 1994; Crocker and Passow, 1995), mesocosm (Dam and Drapeau, 1995) and field experiments (Kiørboe *et al.*, 1995). Coagulation may not only account for the vertical flux of phytoplankton but may also control population dynamics by adding a density-dependent loss term (Jackson, 1990; Kiørboe *et al.*, 1994). Finally, grazing may lead to the sedimentation of phytoplankton through two different pathways. Phytoplankton biomass may sink as fecal pellets or as marine snow generated by zooplankton feeding processes rather than cell-cell coagulation (e.g. Alldredge and Silver, 1988). Marine snow formed from discarded larvacean houses or pteropod webs, for example, may contain phytoplankton cells collected during feeding by the animals or passively scavenged after houses or webs are discarded.

Although sedimentation rates have been measured in many systems (see reviews by Betzer *et al.*, 1984; Wassmann, 1990) the relative roles of the various phytoplankton settling mechanisms have rarely been examined. In this study, we describe the development and sedimentation patterns of a diatom bloom in East Sound on the US/Canadian west coast border with emphasis on the processes controlling the sedimentation and population dynamics of the phytoplankton. Overall sedimentation rates during this bloom were low and mass sedimentation and bloom termination were not observed. Phytoplank-
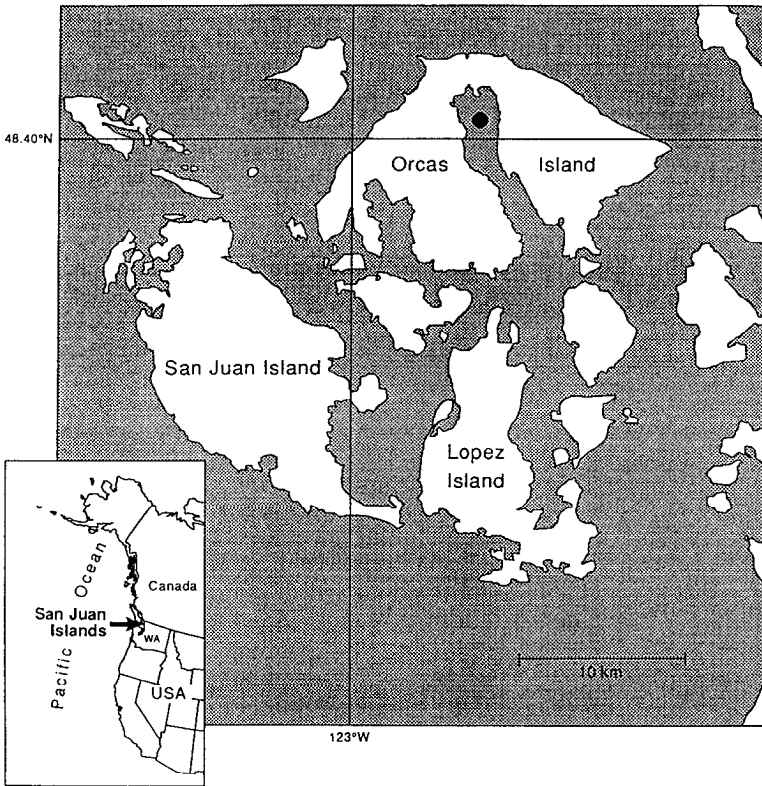
Figure 1. Map of US west coast with detailed map of East Sound.

ton settlement resulted primarily from the sinking of abandoned larvacean houses containing attached cells. Coagulation was unimportant in forming large aggregates and other mechanisms were inadequate to produce rapid mass sedimentation of the bloom.

2. Material and methods

a. Study area and sampling scheme

The study was conducted in East Sound, Orcas Island in the archipelago of the west coast of Washington, USA (Fig. 1) during the period 14–24 April 1994. East Sound is 10 km long and 2 km wide and has a reasonably uniform bottom depth of 28–30 m. All water enters the sound across a narrow sill, 8 to 22 m deep, at the southern end. All sampling was conducted at a 28 m deep station in the middle of the northern portion of the Sound (48° 40′02″N, 122° 54′01″W).

A bottom-mounted acoustic Doppler current profiler (ADCP) (1200 kHz, RD Instruments) was deployed at 48° 40′04″N, 122° 53′72″W between 15 and 22 April. The nominal water depth was 26 m. The instrument sampled horizontal and vertical currents every 1 min at 1 m vertical resolution at distances from 4.2 to 23.2 m above the bottom.

The station was occupied every morning between 0800 and 1000 h and during 19–21 April also between 1800–2400 h. On each sampling occasion a vertical profile of salinity, temperature and fluorescence was first recorded by a Seabird CTD (model SBE19) coupled up with a Seatech *in situ* fluorometer. Subsequently, water was collected by a rosette water sampler (30 l Go-Flo bottles) at 3–5 depths for analysis of bulk water properties. Vertical net hauls (diameter: 50 cm, mesh size: 333 μm) were taken from 7 m above the bottom to the surface. Plankton net tows (20 μm mesh size) were also taken within the uppermost 6 m to collect phytoplankton for stickiness measurements. Finally, sediment traps (see below) were retrieved and redeployed. Samples for nutrients and particulate organic carbon were filtered and stored onboard ship. All other samples were processed at Friday Harbor Laboratory within 2–3 h of collection. Marine snow was collected by divers as described by Alldredge (1992).

b. Nutrients and suspended particles

Nutrients: Duplicate seawater samples from all depths were filtered through a 0.45 μm syringe filter directly into clean 25 ml polyethylene vials and stored frozen at $-30°C$ until analyzed by flow injection for nitrate, silicate, phosphate and ammonium according to Johnson *et al.* (1985).

Particulate organic carbon (POC): Total POC was determined on two replicate 500-ml samples from each depth collected and analyzed according to Sharp (1992) on a Leeman Labs Model CE 440 CHN Analyzer.

Particle concentrations: Particle concentrations were measured on water samples with an Elzone-280 electrical impedance particle counter (Particle Data, Inc.). Samples of 1 and 3 ml were analyzed using 120 and 380 μm aperture tubes, respectively. Results were combined and used to calculate particle size spectra for particles with equivalent spherical diameters (ESD) between 4 and about 100 μm. Further details on the procedure are in Dam and Drapeau (1995) and Jackson *et al.* (1995a).

Transparent exopolymeric particles (TEP): Concentrations of TEP were determined spectrophotometrically from each depth as described in Passow and Alldredge (1995). Four replicate samples of 50–100 ml each were filtered and then stained with Alcian Blue. Gum Xanthan was used for calibration.

Phytoplankton pigments: Phytoplankton pigments were measured at the subsurface fluorescence maximum (4–8 m depth) and at 21 m depth. Between 1000–2000 ml of water were filtered onto 47 mm Whatman GF/C filters, packed in aluminum foil, and frozen.

Within three weeks the samples were extracted in 90% aqueous acetone and analyzed spectrophotometrically at 663 and 480 nm for plant pigments (chlorophyll, phaeopigments, and carotenoids) before and after acidification of the sample (following Strickland and Parsons, 1968 and Heath *et al.,* 1990). The concentration of carotenoids in phytoplankton cells is largely independent of the ambient nutrient conditions, while chlorophyll decline when cells are nitrogen starved. The ratio of absorbencies at 480 (carotenoids) and 663 (chlorophyll) nm is therefore a measure of nitrogen limitation; ratios exceeding 2.0 suggest

nitrogen limitation (Heath *et al.,* 1990). Pigment analyses were also used to calibrate the *in situ* fluorometer, and a regression between pigment concentration (chlorophyll + phaeopigment) versus fluorometer reading was established ($r^2 = 0.85; n = 25$).

Phytoplankton cell counts: 100–500 ml of sample from the fluorescence maximum (4–8 m depth) and 21 m depth each were preserved with acid Lugol's solution (10 ml/l of sample). Diatoms, dinoflagellates and *Phaeocystis* cells (but not other small flagellates) were counted in 5 or 10 ml subsamples (inverted microscope); at least 400 diatom cells were counted in each sample. In addition, large (>75 μm disc diameter) *Thalassiosira* sp. cells were counted in four 10-ml subsamples under the dissecting microscope (~50–700 cells per sample). Diatoms were determined to species or genus. Care was taken to categorize cells into different species, even in cases where the correct name could not be provided. The *Thalassiosira* group was particularly difficult in this respect and scanning micrographs were, therefore, prepared to help light microscopical classification. On this basis three *Thalassiosira* groups were distinguished; viz <25 μm (one species), 25–75 μm (about 3–4 species that could not be separated in the light microscope), and >75 μm (*Thalassiosira mendiolana*). Cell and plasma volumes for each species were obtained from linear cell measurements by assuming simple geometrical shapes as described in Anon (1988); phytoplankton carbon was estimated from plasma volumes assuming 0.11×10^{-6} μg C μm^{-3} (Strathmann, 1967). Fecal pellets (of mainly copepods) were concentrated on a 40-μm sieve and counted in the entire sample under the dissecting microscope. Linear dimensions of 30 pellets were measured and their volumes calculated assuming cylindrical shape. Carbon content of fecal pellets was estimated by assuming a carbon:volume conversion of 0.11×10^{-6} μg C μm^{-3} (Smetacek, 1980).

Zooplankton counts: All zooplankton samples were preserved in alcohol (70%). Later, samples from net-tows of the morning stations were counted with a dissecting scope.

Marine snow: Visible aggregates were collected in hand-held syringes by divers on April 19, 20, 21, 23 and 24 at 5, 10 and 20 m depths. A known number of aggregates was collected in each syringe (typically 10 or 20, but up to 100). In the lab the contents of the syringes were preserved with formalin (2%). Phytoplankton and fecal pellets were counted under the inverted microscope in the entire sample or in subsamples as above. Phytoplankton per aggregate was calculated after subtraction of ambient phytoplankton concentration. TEP concentration was also measured.

c. Sedimentation rates and settling velocities

Sediment traps: The sediment trap was deployed at 21 m depth and consisted of 6 individual trap-tubes (inner diameter: 65 mm, height: 675 mm height). The top 100 mm of each tube consisted of 7 baffle tubes, each measuring 17.5 mm inner diameter (21.5 outer diameter). Traps were retrieved approximately every 12 or 24 h.

Two of the six trap tubes were equipped with a petri-dish on the bottom which contained an 8% polyacrylamide solution to collect intact aggregates (Lundsgaard, 1996). A varying number of the baffle-tubes were closed by stoppers to reduce the amount of material in the

traps. The baffles were stopped from below, and material settling in the 10 cm deep baffle tubes was not resuspended. The trapping area was, thus, reduced proportionally to the area of the stopped baffles. This was verified in one instance in which a different number of baffles were closed (corresponding to 15 and 54% reduction in area) in replicate traps; the two traps yielded flux estimated differing by less than 2%. Aggregates were counted and sized from photographs of the petri dishes as described and reported in further detail by Hansen *et al.* (1996), and the daily volume flux of aggregates (as ml m^{-2} d^{-1}) was calculated. The contents of three tubes (each 1.8 l) were used for replicate analysis of POC, TEP, phytoplankton pigments and cells as described above. Fecal pellets in trap material were too disintegrated to allow quantification. In calculating fluxes, we subtracted the background concentration of pigment or cells at 21 m depth, estimated as the average concentration at the beginning and end of the deployment period.

Phytoplankton sinking velocities: Settling velocities of suspended particulate phytoplankton pigments from the surface morning samples were measured daily in a setcol-setup (Bienfang, 1981b). Prior to incubation, particles in the water samples were concentrated about 5–10 times by inverse filtration on 6 μm plankton gauze. Samples were filtered onto 25 mm GF/C filters, frozen, and later extracted in 90% acetone and measured on an AMINCO colo-fluorometer.

d. Assessment of coagulation processes

Rates of particle aggregation via processes of coagulation are dependent upon the abundance and size distribution of aggregating particles, the intensity of the shear colliding them together and the stickiness of these particles once collided. We assessed these factors to evaluate the role of coagulation in sedimentation of the bloom.

Shear: Horizontal currents determined with the ADCP were digitally filtered with a 7-point Butterworth filter having a cutoff frequency of 7.5 cycle h^{-1} and then used to calculate bulk shear rates through the water column. Further shear can arise from turbulent motions induced by the larger scale water motions if the density stratification is suitably small. This turbulent shear rate can be estimated from average shear and vertical density structure (Mellor and Yamada, 1982). We used the equations of Sharples and Tett (1994) to attempt to estimate the turbulent motions. However, we were unable to distinguish any additional shear from statistical artifacts associated with noisy density profiles.

Particle stickiness: The tendency of particles to form aggregates by coagulation was examined by measuring the probability that two particles will stick together upon collision (their 'stickiness') in a Couette device by the method of Kiørboe and Hansen (1993) and Drapeau *et al.* (1994). The procedure allowed particle suspensions to aggregate in the annular gap between two cylinders, the outer one rotating, while the decline in particle number concentration due to aggregation was monitored using the Elzone particle counter (380 μm aperture). Particle stickiness can be estimated from the slope of the exponential decline of particle number (Kiørboe *et al.*, 1990). Particle stickiness was measured daily in field samples between 17–24 April. Particles (>20 μm) were collected with net plankton

tows, except on April 24 when seawater was collected with a Go-Flo bottle from 6 m. Experiments were run at a concentration of around 30 ppm, except on 24 April when 15 ppm was used. Shear rate was 5.7 s^{-1}. Experiments were run in duplicate following the procedure of Dam and Drapeau (1995).

The diatom *Thalassiosira mendiolana* dominated the phytoplankton biomass that developed in East Sound. We therefore isolated this species from 20-μm net hauls taken on April 23. The cells were then grown in batch cultures in B$_1$-medium (Hansen, 1989), constant light ($\sim$100 μE m^{-2} s^{-1}) and at 16°C. Cell stickiness was measured at about 2 d intervals as the culture developed following a protocol similar to that described in Kiørboe and Hansen (1993).

Coagulation rate estimates: We calculated the instantaneous coagulation rates for particle size spectra derived from the Elzone particle counter using the methods of Jackson (1995a). The resulting rates were normalized by the particle size spectra to yield net specific rates of change as a function of particle size. The particles were assumed to have a fractal dimension of 3, with the collisions being described by curvelinear coagulation kernels.

3. Results

a. Physical environment

The water column in the Sound was vertically stratified due to both temperature and salinity differences, although the temperature effect was greater (Fig. 2). The pycnocline was located at about 5 m. Heating of the surface layer increased the temperature of the near-surface region over the course of the field program. Subsurface temperatures varied relatively little during this time. There were small changes in subsurface salinity on 19 and 21 April.

The average currents were small over the course of the experiment with most of the energy at tidal frequencies. The RMS currents were 2–3.5 cm s^{-1}, with the highest values near the surface (Fig. 3). The residual currents were weak, with mean values of 0.5–1.5 cm s^{-1} to the northeast. The average shear was small, ranging from about 0.01 s^{-1} within 15 m of the bottom to slightly more than 0.02 s^{-1} near the surface (Fig. 3).

b. Development of the bloom

Field studies of phytoplankton population dynamics require that the same populations are sampled during the entire study. Because there were no abrupt changes in either water column structure or in phytoplankton species composition or abundance and because residual currents were very low, we conclude that advection was occurring at a spatial scale which was less than the distribution of the considered populations.

Phytoplankton: We observed a diatom bloom develop during the study period. Total chlorophyll *a* was high, reaching 20 μg l^{-1} at the termination of observations. Chain-forming species dominated the diatom community numerically, particularly *Chaetoceros*
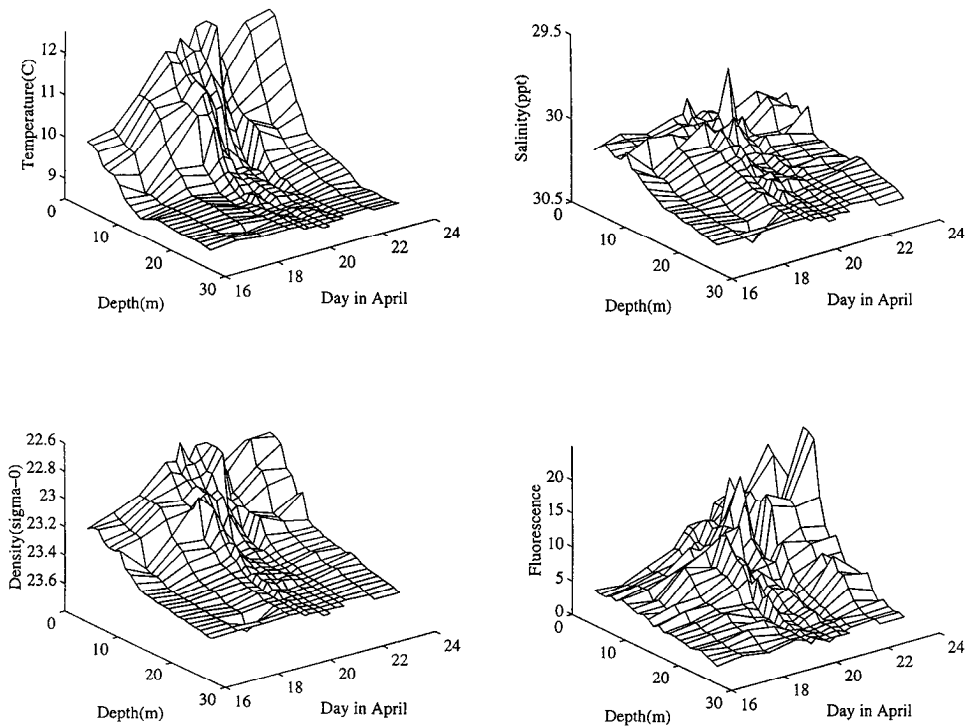
Figure 2. Vertical and temporal variation in salinity, temperature, density and fluorescence at the sampling station between April 14–24.

spp. (*C. danicus, C. debilis, C. socialis* and at least 7 other species), followed in abundance by *Thalassiosira* spp., *Pseudonitzschia* sp., *Thalassionema nitzschioides, Nitzschia* spp. and *Rhizosolenia* spp. that each contributed on average 5–17% of diatom abundance in the surface samples (Fig. 4), and between 3–23% in the deep samples (not shown). However, in terms of biomass *Thalassiosira* spp. accounted for on average 77% of the diatom carbon in surface water (Fig. 4), and the solitary *Thalassiosira mendiolana* (about 75 µm diameter) was the most important individual species, contributing from ca. 10% of the carbon-biomass at the beginning of the period to 50–75% later. Phytoplankton other than diatoms included *Phaeocystis pouchetti* (up to 3000 cells ml^{-1}), the concentration of which did not change systematically during the period, and dinoflagellates, mainly *Ceratium fusus,* which occurred in low concentrations (<8 cells ml^{-1}) throughout.

Phytoplankton biomass, measured both as concentration of pigments (chlorophyll + phaeopigment) and as total phytoplankton carbon (from cell counts), began to increase exponentially subsequent to April 17 at an average net rate of about 0.2 d^{-1} in surface water (Fig. 5). Net growth rates of different species, however, varied appreciably, ranging from the high rates of *Thalassiosira mendiolana* (0.31 d^{-1}) to low rates of other diatoms (average 0.11 d^{-1}) (Fig. 5) or *Phaeocystis pouchetti* (~0 d^{-1}). There was no indication that
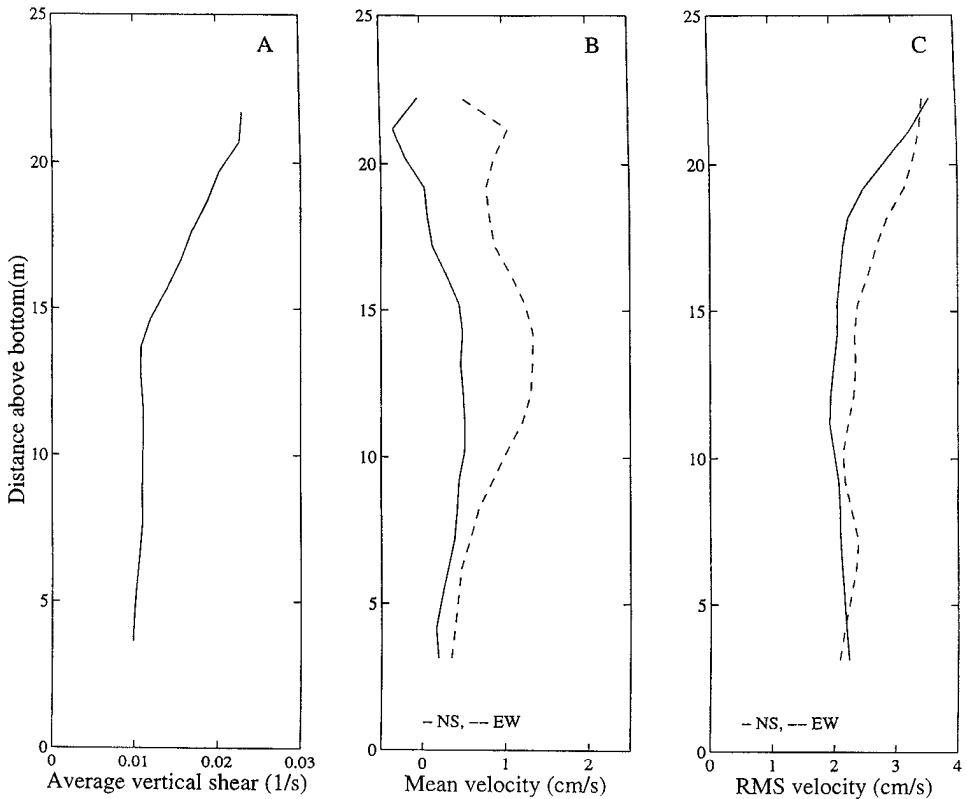
Figure 3. Distribution of (A) average shear; (B) Mean velocity; (C) RMS velocity through the water column. Values were estimated from ADCP profiles and are given as a function of distance above the bottom. In (B, C) solid lines are N(+)S currents and dashed lines are E(+)W currents.

growth had ceased when observations were terminated. Phytoplankton concentrations at 21 m largely followed those in the surface samples, but were on average only about half of those.

The concentration of phytoplankton carbon (from cell counts) varied linearly with phytoplankton pigment concentration, and the relations were similar for the surface and the 21-m samples. We, therefore, calculated a common regression (Fig. 6). The slope of this regression is a measure of the phytoplankton carbon:pigment ratio and the estimate of 24 is typical for healthy diatoms. The ratio of carotenoids to chlorophyll, as assessed by the absorption ratio (A_{480}/A_{663}), also remained constant during the study period with a value close to 1.0 (average 1.06 ± 0.06; range 0.9–1.2), suggesting that the cells never became nutrient limited. This is consistent with the high concentration of inorganic nutrients in surface waters throughout the study period; SiO_4 remained >10 µM, PO_4 > 1 µM, and NO_3 > 5 µM. Thus, there were no signs of limitation by major nutrients, phytoplankton senescence, or termination of the bloom, even at the end of the study period.
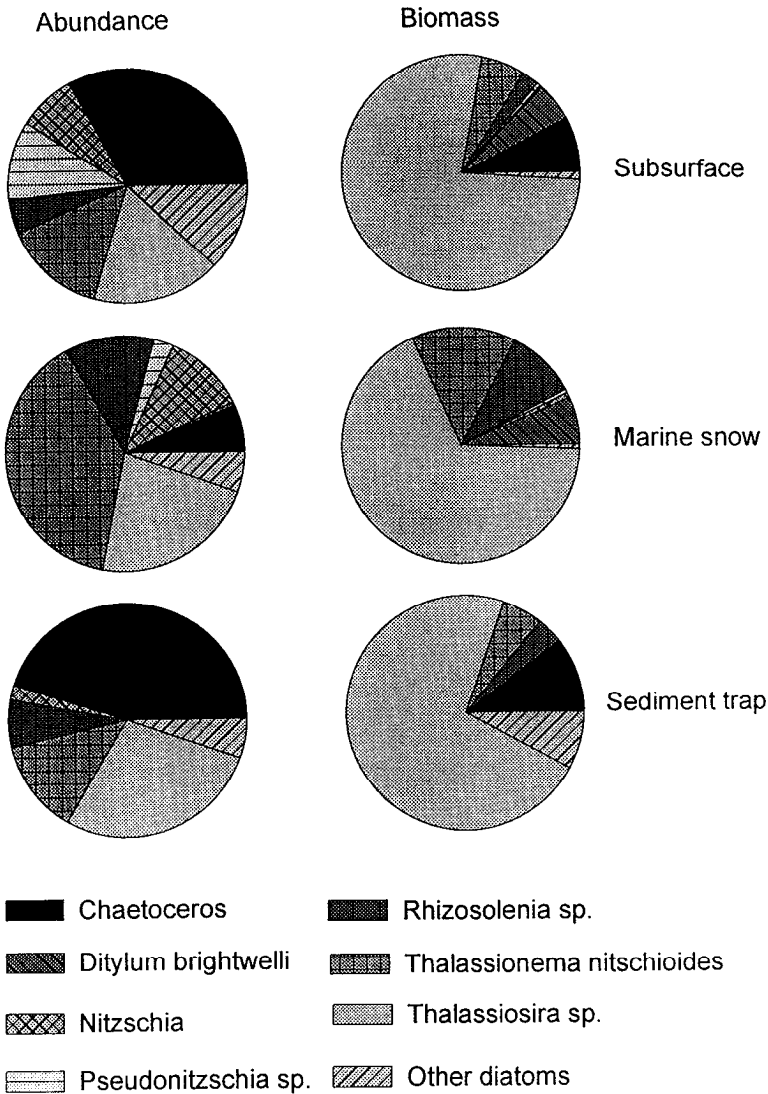
Figure 4. Composition of the diatom community at the sampling station in surface water, marine snow aggregates, and in sediment traps. (A) Average relative abundances of main diatom groups; (B) Average relative biomass of main diatom groups.

POC and TEP: The concentration of POC varied in concert with phytoplankton (Fig. 7A) but variations were damped due to a high background concentration of (presumably detrital) POC. Plots of POC vs. phytoplankton pigment (POC = 225 + 24.2 × pigment; $r^2 = 0.74$) and phytoplankton carbon (from cell counts) (POC = 252 + 0.72 × Phyto-C; $r^2 = 0.58$) (all units in µg l^{-1}) yielded estimates of this background concentration of 225–250 µg C l^{-1} (ordinate intercepts). As a consequence,
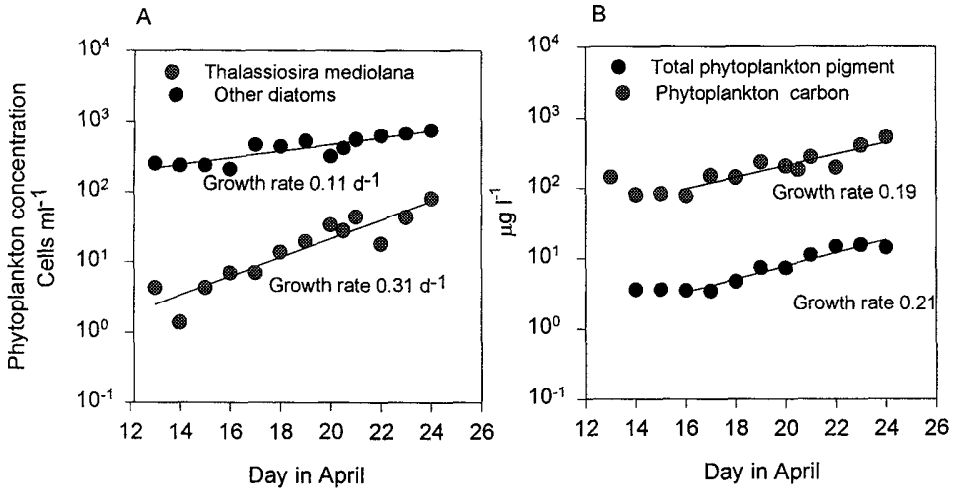
Figure 5. Temporal development in concentrations (cells ml^{-1}) of *Thalassiosira mendiolana* and other diatoms (A), and in concentrations (mg l^{-1}) of phytoplankton pigment and phytoplankton carbon (B) in subsurface samples. Average growth rates (from regressions) have been shown for each property.

phytoplankton carbon accounted for only 20% of POC in the beginning, but increased to ca. 75% by the end of the study period. The estimated carbon to pigment ratio (slope of POC vs. pigment), 24.2, is consistent with the above estimate based on cell counts. Concentrations of TEP increased simultaneously with Chl *a* during the second half of the
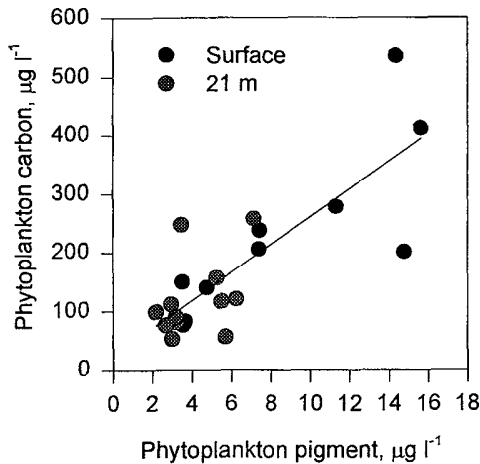

Figure 6. Concentration of phytoplankton carbon (C, mg Carbon l^{-1}, from cell counts) vs. concentration of phytoplankton pigment (P, mg pigment l^{-1}) for subsurface (filled symbols) and 21-m samples (open symbols). Common regression (not shown) is $C = 23.7 \times P + 24.0$, $r^2 = 0.65$, $n = 23$.
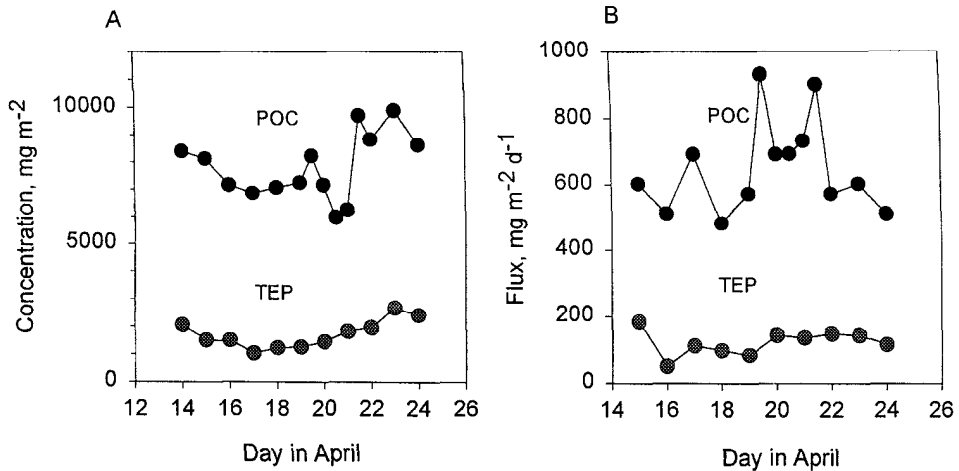
Figure 7. Concentration and flux of POC and TEP. (A) Concentrations of particulate organic carbon (POC) and transparent exopolymer particles (TEP); (B) Sedimentation rates of POC and TEP. TEP are in units of Xanthan equivalents.

study period (Fig. 7A). However, concentrations of TEP were low (50–160 μg Xanthan equiv. per liter) in relation to Chl *a* values, which suggests that dominating phytoplankton species did not generate TEP abundantly. TEP concentrations in marine snow were also very low (0.7–2.3 μg Xanthan equiv. per aggregate) compared to the amount of TEP found in aggregates formed by coagulated phytoplankton (Monterey Bay, June/July 1993 and Santa Barbara, September 1994: ≥6 and ≥7 μg Xanthan equiv. per aggregate respectively, unpubl.).

Marine snow: All marine snow particles observed and collected by divers consisted of abandoned larvacean houses to which phytoplankton cells, fecal pellets and detritus had become attached. The taxonomic composition of the phytoplankton associated with these aggregates differed from that of the ambient water mainly in that *Chaetoceros* spp. was underrepresented in the aggregates. In terms of biomass, *Thalassiosira* spp. was dominant (Fig. 4). There was no consistent temporal variation in the amount of phytoplankton attached to snow particles, but particles collected deeper had higher concentrations than those collected near the surface. Average phytoplankton carbon per aggregate (from cell counts) were 0.28 ± 0.16, 0.53 ± 0.31 and 0.57 ± 0.12 μg C at 5, 10 and 20 m depth, respectively. The average volume of diver-collected snow particles was 1 μl (Hansen *et al.*, 1996), and the concentration of phytoplankton in the aggregates was, therefore, on the order of 0.5 μg C μl^{-1}. This is about three orders of magnitude higher than ambient concentrations. A more detailed account is given in Hansen *et al.* (1996).

Zooplankton and fecal pellets: Zooplankton abundance was nearly constant at 2000 to 3000 animals per m^3 throughout the study and was dominated by Copepods, primarily of the genus *Acartia* (Fig. 8A). The larvacean *Oikopleura dioica,* ostracods, the medusa *Eucoria victoria,* and a variety of crustacean larvae were also present. The concentration of
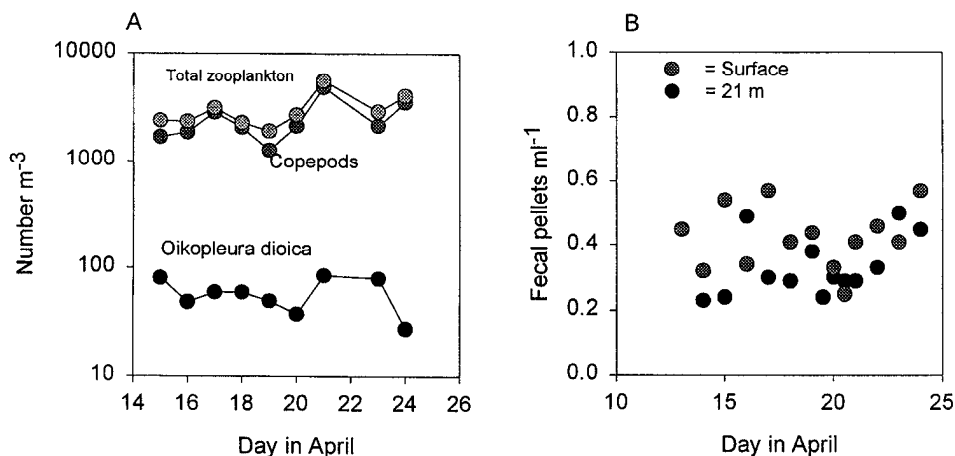
Figure 8. Zooplankton parameters (A) Abundance of important zooplankton taxa; (B) Concentration of copepod fecal pellets in subsurface and 21-m samples.

zooplankton fecal pellets was also almost constant during the study period, 0.42 ± 0.10 and 0.33 ± 0.09 ml^{-1} in surface and 21-m samples, respectively (Fig. 8B). The almost constant concentrations of zooplankton and pellets suggest that grazing pressure did not change much during the study period. Pellets varied in length between 30–180 µm and in width between 20–70 µm; average fecal pellet volume was 1.3×10^5 µm^3, equivalent to 1.5×10^{-2} µg C pellet^{-1}. Fecal pellet carbon concentration (~ 5 µg C l^{-1}) was, thus, small compared to that of the phytoplankton.

c. Vertical flux

   Description of settled material: The phytoplankton composition of major taxonomic groups in the trap samples was similar to the composition in the water column except that the genera *Nitzschia* and *Pseudonitzschia* were almost absent in the trap samples; again *Thalassiosira* spp. was dominant in terms of biomass (Fig. 4).

   The petri dishes filled with polymer allowed us to examine the 3-D organization of the settled material under the dissecting microscope. Most settled material was associated with 1–3 mm-diameter aggregates. The majority of these aggregates were abandoned larvacean houses to which live phytoplankton cells, fecal pellets and detrital material were attached. Phytoplankton cells associated with the aggregates were mainly chain-forming *Thalassionema nitschioides* and *Thalassiosira* spp., including the solitary *Thalassiosira mendiolana*. Many phytoplankton cells were not attached to aggregates. It was not obvious to what extent these cells had been detached from aggregates as these sank through the polymer or to what extent they had arrived in the trap independent of an aggregate. We did not observe distinct phytoplankton aggregates at any time.

   Vertical flux and sinking velocity of particulate pigment and phytoplankton carbon: The sedimentation rate of particulate pigment was relatively constant throughout the study
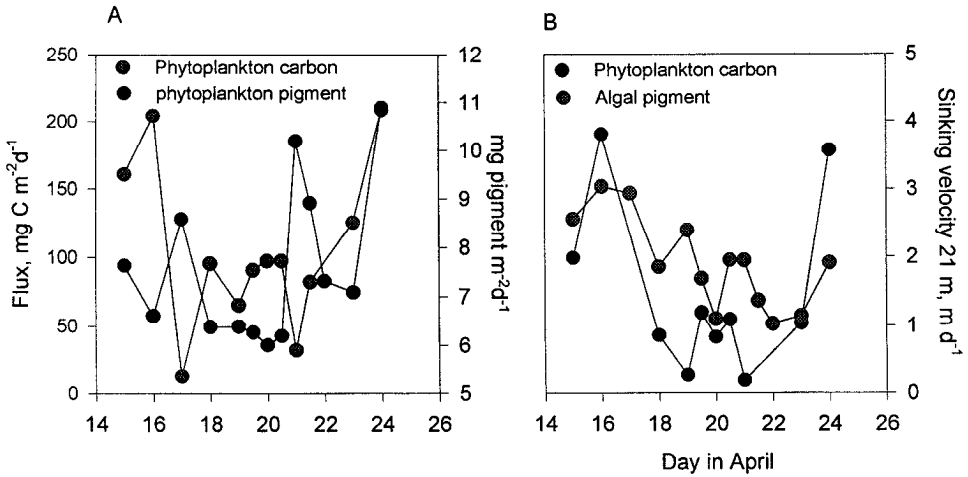
Figure 9. Vertical flux (A) and sinking velocities at 21 m (B) of phytoplankton pigment and carbon.

period, between 6 and 10 mg pigment m^{-2} d^{-1} (Fig. 9A), whereas the flux of phytoplankton carbon calculated from cell counts varied considerably more, 10–200 mg C m^{-2} d^{-1} (Fig. 9A). As a consequence, the phytoplankton carbon to particulate pigment ratio in the settled material was more variable and on average significantly less than in the suspended particulate material (average ± SD = 14.6 ± 8.0). This discrepancy may be due to sedimentation of pigment in fecal pellets, and the difference would suggest that about one third of the settled pigment was in fecal pellets. Pigment flux as a fraction of integrated pigment concentration in 0–21 m (calculated from calibrated *in situ* fluorometer readings) averaged 9.9 ± 3.9% d^{-1}.

Average settling velocity (m d^{-1}) of particulate pigment and phytoplankton carbon at 21 m depth, calculated as the ratio of sedimentation rate (mg C m^{-2} d^{-1}) to concentration at 21 m (mg m^{-3}, measured at retrieval of trap) are presented in Figure 9B. Average settling velocities of pigment and phytoplankton carbon varied in concert, between 0.2–4.0 m d^{-1}. However, the sinking velocity of pigments was generally faster and less variable than the sinking of phytoplankton carbon (from cell counts). This may be due to an almost constant background sedimentation of pigments in fecal pellets with high settling velocities.

Settling velocities of particulate pigment as determined by SETCOL incubations of surface water samples (Fig. 10) were almost an order of magnitude less than those inferred from *in situ* by traps at 21 m depth, 0.2–0.5 m d^{-1}. There was no obvious temporal pattern in SETCOL settling velocities. The higher and more variable settling velocities calculated from *in situ* measurements may be due to the formation of rapidly sinking aggregates.

Flux of aggregates: The volume flux of aggregates varied by about an order of magnitude during the observation period (Fig. 11). The temporal variation in sinking velocity of phytoplankton carbon and, to a lesser extent, particulate pigment resembled the temporal variation in sedimentation of aggregates (compare Figs. 9 and 11), and there was
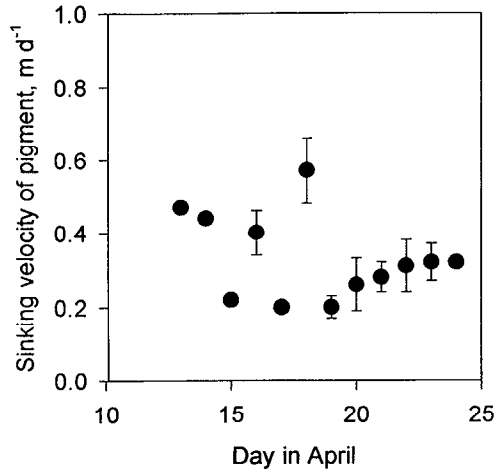
Figure 10. Sinking velocities of particulate phytoplankton pigment in subsurface samples as determined in SETCOL incubation experiments. Average ± SD of replicate experiments.

a good correlation between aggregate flux and phytoplankton sinking velocity (Fig. 12). This suggests that fallout of phytoplankton attached to rapidly sinking larvacean houses was important for driving phytoplankton sedimentation in East Sound during the study period.

We examined this further by comparing the observed flux of phytoplankton carbon (from trap cell counts) with that predicted from the flux of aggregates multiplied by the amount of phytoplankton per aggregate. We used estimates of phytoplankton-carbon per aggregate as measured in the aggregates collected by divers at 20 m depth assuming an average size of 1 µl per aggregate (Hansen *et al.*, 1996) (Fig. 13A). We also used estimates
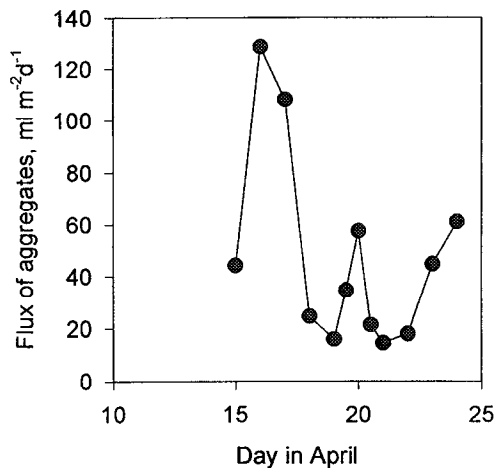

Figure 11. Volume flux (μl m^{-2} h^{-1}) of aggregates at 21 m depth as determined in sediment traps.
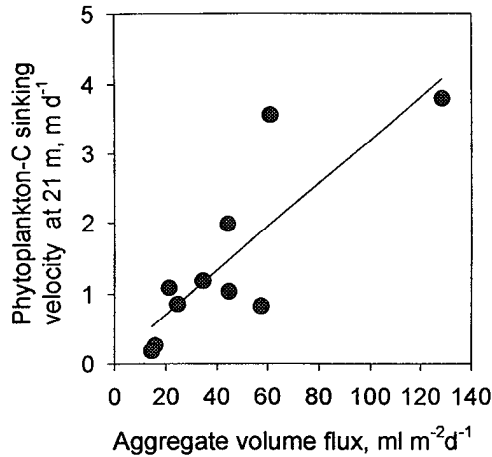
Figure 12. Phytoplankton settling velocity as determined from cell counts versus vertical volume flux of aggregates. $r^2 = 0.69$ and $n = 10$ of the shown regression line.

of the abundance of specific plankton components as measured in aggregates collected in the polymer (Hansen *et al.*, 1996) (Fig. 13B). Both approaches yielded fair correlations. The slopes of the regressions (0.15–0.26) indicate the fraction of phytoplankton that sediments in association with aggregates (i.e. 15–26%). We suspect that these fractions are underestimates, because if only 15–26% of the sedimenting phytoplankton is associated with aggregates, the relationships should not be as strong as those actually observed.

Flux of TEP and POC: Fluxes of both POC and TEP varied only little temporarily (Fig. 7B), were unrelated to fluxes of phytoplankton, and averaged $8.1 \pm 2.1\%$ d^{-1} and $7.6 \pm 2.8\%$ d^{-1} of the standing stocks.

d. Coagulation processes

Phytoplankton stickiness: The measured stickiness of particles that were retained in a 20-µm plankton net varied between $-0.01–0.17$ and averaged 0.048 ± 0.067 ($n = 14$), implying that on average only 4.8% of collisions resulted in sticking of the colliding particles. Average of stickiness measurements was greater than 0.1 on only one day (April 20). Results of all other measurements suggest very low or zero stickiness.

The stickiness of *Thalassiosira mendiolana* grown in batch culture was low and on average not significantly different from zero (average $\pm$ SD: -0.001 ± 0.027; $n = 12$). Also, there was no obvious change in stickiness as the culture aged and the cells became nutrient limited (Fig. 14). We conclude that the stickiness of both *Thalassiosira mendio-lana*, the dominant phytoplankter, and of naturally occurring particles was low enough to be indistinguishable from zero.

Coagulation rates: We calculated the specific rate of change of particle concentration due to coagulation for the particle spectrum with the highest particle concentrations (surface sample on April 24; Fig. 15A) assuming a shear rate of 0.02 d^{-1} (Fig. 3) and a
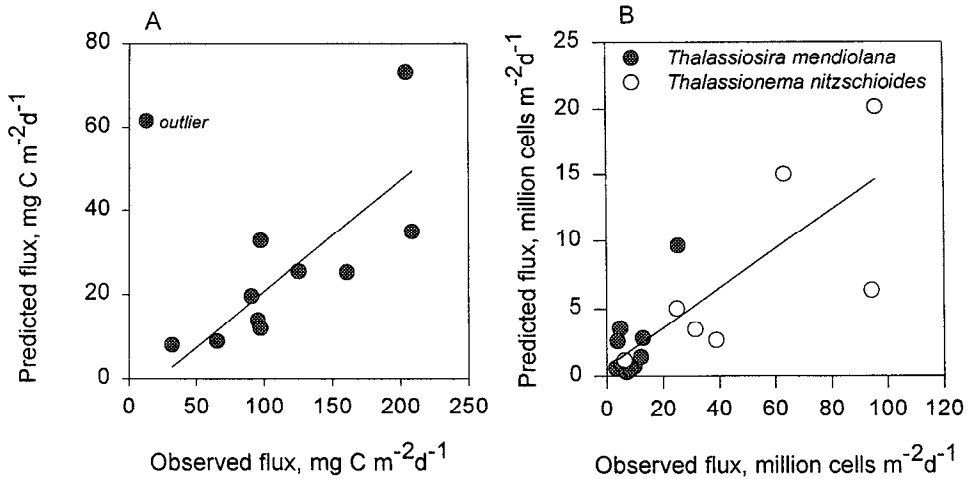
Figure 13. Observed flux of phytoplankton compared to that predicted from the vertical flux of aggregates. (A) sedimentation rate of phytoplankton carbon predicted from volume flux of aggregates multiplied with the volume-specific content of phytoplankton carbon in aggregates collected by divers at ca. 20 m depth. The regression between predicted and observed flux, excluding the one outlier, has a slope of 0.26 and $r^2 = 0.62$, $n = 11$. (B) sedimentation rate of *Thalassiosira mendiolana* and *Thalasionema nitschioides* predicted from volume flux of aggregates multiplied with the volume- and time-specific contents of the two species in aggregates collected in polymer in sediment traps (from Hansen *et al.,* 1996). The regression between predicted and observed flux has a slope of 0.15, $r^2 = 0.64$, $n = 17$.

stickiness of 0.05. Because collision frequencies and, thus, coagulation rates depend on particle concentration squared this is a maximum estimate. The calculation showed a maximum decrease of $0.07 \, d^{-1}$ associated with the spectral peak at 40–50 μm ESD (Fig. 15B), which corresponds to the dominating diatom (ca. 75 μm disc diameter). Specific decrease rates were even slower for smaller particles. Note that this calculation indicates only the instantaneous change in aggregation rate. However, the calculation does indicate that coagulation was a relatively slow process that would have had a small effect on the particle size spectra for the observed conditions. The principal reason for this low aggregation potential was the small values of particle stickiness.

4. Discussion

Although a very large phytoplankton biomass concentration developed in East Sound, no large sedimentation event terminated the bloom during our study period. The constant sedimentation rates of POC, TEP, Chl *a* or cells, low relative to respective standing stocks, indicate that mass sedimentation was not occurring. It is generally believed that diatom blooms are terminated by coagulation of cells and subsequent mass sedimentation of these aggregates. In the following discussion we try to assess in detail which mechanisms were
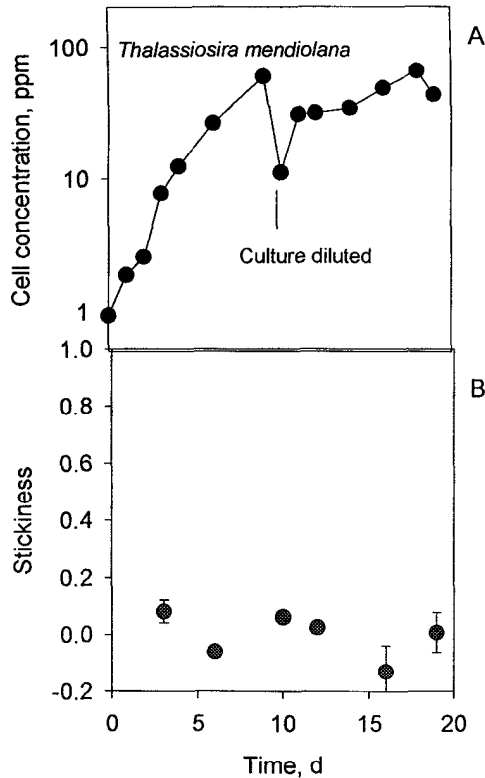
Figure 14. Stickiness of the diatom *Thalassiosira mendiolana* grown in batch culture. Temporal development of concentration (A) and stickiness (±SD) (B) of *T. mendiolana* as the batch culture ages. On day 10 the culture was diluted with growth medium.

responsible for the ongoing low sedimentation and to evaluate the degree to which the bloom size was regulated by sedimentation.

The flux (F) of phytoplankton relates to the abundance of phytoplankton (B) in the water column depending on the mode of sedimentation. The relationship between F and B may be described by a power function

$$F = aB^b$$

and the magnitude of b for a set of observations is related to the removal mechanism. A value of $b > 1$ would be consistent with coagulation as a dominant removal mechanism; model calculations of Farley and Morel (1986) and Burd and Jackson (1996) suggest that $1.2 \leq b \leq 2.1$ if coagulation dominates. A value of $b \sim 1$ suggests that the phytoplankton sediments mainly as individual cells or chains because a constant fraction of phytoplankton will settle out per unit time if the buoyancy and sinking velocity are independent of the phytoplankton concentration. A value of $b < 1$ would finally suggest that other processes that are less dependent on phytoplankton biomass drive the sedimentation. This could be
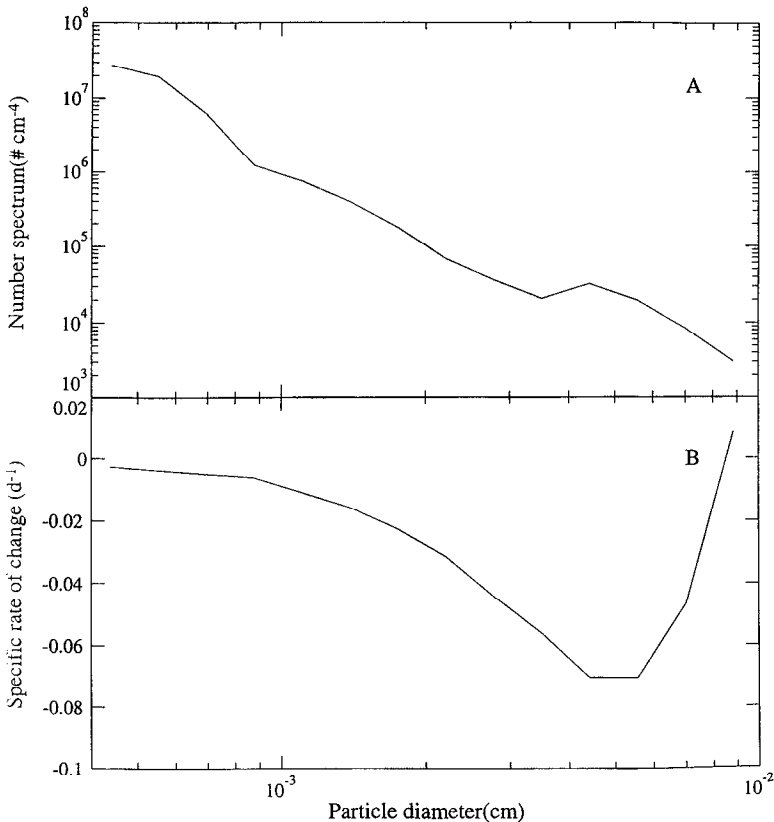
Figure 15. Particle size spectra (A) and predicted change in concentration (B) for near-surface samples collected on 24 April. These had the highest particle concentrations of water sampled during the program.

grazing in a broad sense (e.g., either sedimentation of fecal pellets or larvacean houses with attached phytoplankton) provided there are no functional and numerical responses in grazing rate to variations in phytoplankton biomass on short time scales of hours to days. Flux and phytoplankton biomass, expressed as either pigment or carbon (calculated from cell counts), for East Sound had insignificant correlations and slopes that do not differ significantly from zero (Fig. 16).

a. Significance of coagulation

Several pieces of evidence indicate that coagulation was unimportant as a mechanism of sedimentation of the bloom in East Sound. First, no relationship exists between flux and suspended biomass of phytoplankton in East Sound during the study period. A similar plot of flux vs. biomass for a diatom bloom occurring in a shallow Danish fjord (Isefjord) where
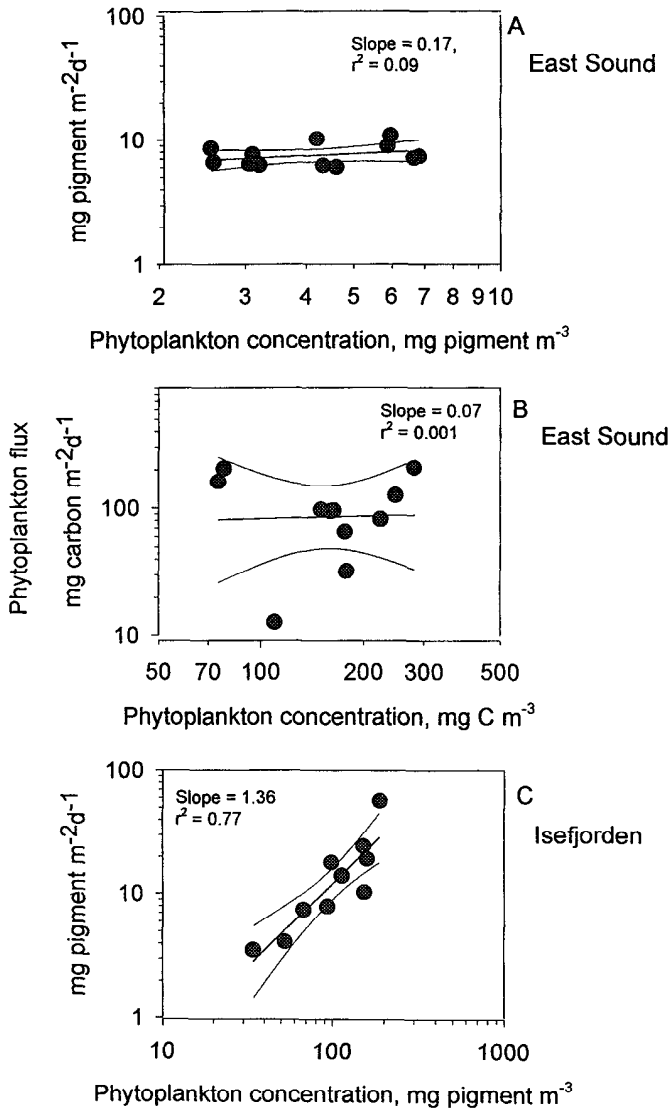
Figure 16. Sedimentation rate vs. suspended biomass in East Sound (A, B) and in Isefjord (C). The units are phytoplankton pigments, as determined spectrophotometrically, or phytoplankton carbon, as determined from cell counts. Slope and r^2 shown for each logarithmic regression. Data for panel C stems from Kiørboe *et al.* (1994).

coagulation was shown to be important (Kiørboe *et al.*, 1994) had a slope ($b = 1.36$) that was within the predicted range of 1.2–2.1 (Fig. 16C).

Secondly, the calculated concentration changes associated with coagulation rates are small relative to growth rates, being at most 0.07 d^{-1}, compared to the 0.31 d^{-1} net growth

rate of the dominating algal cells. The low calculated coagulation rate was the result of the low stickiness value. This calculation even overpredicts the significance of coagulation and is, thus, conservative relative to the conclusion that coagulation was unimportant because: (i) the calculation is based on the highest particle concentration measured; (ii) the calculation suggests that coagulation was due primarily to the 40–50 μm ESD size class, which corresponds to the dominant diatom, *Thalassiosira mendiolana,* that was not sticky at all. A sensitivity analysis showed that varying the shear had little effect because differential settling was the dominating collision mechanism in this system. Thus, abundance and in particular stickiness of the phytoplankton was insufficient for phytoplankton coagulation to be important for sedimentation and population regulation during this diatom bloom.

A third piece of evidence that coagulation was unimportant is that the concentration of TEP was low throughout the bloom in relation to concentrations seen in other natural blooms undergoing mass flocculation and sedimentation (Passow *et al.,* 1994; Passow and Alldredge, 1995a). It has been argued that algae producing TEP are sticky (Dam and Drapeau, 1995) and that abundant TEP is necessary for most diatom blooms to aggregate (Logan *et al.,* 1995), although the exact mechanism for this is unclear (Jackson, 1995b). Finally, aggregates collected by divers and collected in polymer-traps were almost invariably larvacean houses and phytoplankton aggregates were not observed.

b. Significance of cell sinking

Sinking velocities of unaggregated particulate pigment was assessed by the SETCOL technique. *In situ* concentrations of aggregates were $<0.5 \, l^{-1}$ (Hansen *et al.,* 1996). Because the samples were shaken before incubation in the 0.5 l SETCOL chambers, we consider the settling velocities estimated this way as representative of unaggregated particles, mainly phytoplankton cells. Our observations suggest that sedimentation of unaggregated cells contributed only marginally to bulk phytoplankton flux because: (i) SETCOL settling velocities were about six times less than pigment settling velocities estimated from trap data (averages were 0.3 ± 0.1 and $1.9 \pm 0.7 \, m \, d^{-1}$, respectively); this would suggest that unaggregated particulate pigment would account for at most 15% of the pigment flux. (ii) The SETCOL estimates suggest that settling velocities of unaggregated particles were constant, or at least independent of suspended biomass during the study period. This would imply an exponent, b, close to 1 provided flux of unaggregated particles was important. (iii) The genus *Chaetoceros,* which dominated the phytoplankton community numerically, hardly occurred in the aggregates, neither in those collected by divers (Fig. 4) nor in those collected in the polymer, yet occurred abundantly in the traps. This would suggest that *Chaetoceros* spp. were settling independently of aggregates. However, since *Chaetoceros* spp. contributed less than 10% of the diatom biomass, they affected the bulk phytoplankton flux relatively little.

c. Significance of fecal pellets and copepod grazing

Copepod grazing contributes, of course, not to the vertical flux of live cells, but may transport phytoplankton material packed in fecal pellets to the sea floor. Fecal pellets in the traps could not be counted and their sedimentation rate, thus, not quantified. However, crude estimates of the quantitative importance of copepod grazing as a sink for the phytoplankton and fecal pellets as vehicles for the vertical material flux can be derived as follows. Fecal pellets of sizes comparable to those occurring here (average volume 1.3×10^5 μm^3) sink at between 10–20 m d^{-1} (Butler and Dam, 1994). Because the abundance of fecal pellets was constantly about 0.4 ml^{-1} (Fig. 8B) the vertical flux of pellets is on the order of 50–100 mg C m^{-2} d^{-1} (pellet concentration $\times$ carbon per pellet $\times$ sinking velocity). This corresponds to about 50–100% of the average phytoplankton carbon sedimentation rate during the study period (107 mg C m^{-2} d^{-1}), and copepod fecal pellets would thus account for on average 30–50% of the vertical carbon flux. This estimate is consistent with the phytoplankton carbon to pigment ratio in the settled material, but may represent an overestimate of the pellet-carbon actually reaching the sea floor, because pellets are degraded and loose solute material as they sink (e.g. Smetacek, 1980; Jumars *et al.,* 1989; Noji *et al.,* 1991). If one further assumes a copepod assimilation efficiency of 67% (e.g. Conover, 1978; Kiørboe *et al.,* 1985), implying that 33% of the ingested carbon is turned into fecal pellets, then the copepod grazing rate is about three times the pellet flux; i.e., 150–300 mg C m^{-2} d^{-1}, or 7.5–15 mg C l^{-1} d^{-1}. This amount represents about 10% of the phytoplankton standing stock d^{-1} in the beginning of the observation period and only 2% by the end. Copepod grazing and sedimentation of intact cells, thus, represent losses to the phytoplankton populations of similar magnitudes.

With an average diatom net population growth rate of 0.2 d^{-1} and losses due to copepod grazing and sedimentation each yielding mortality (loss) rates of up to 0.1 d^{-1}, the phytoplankton must have had an average gross population growth rate of about 0.4 d^{-1}. This is similar to what has been observed in other temperate waters during spring blooms where grazing and sedimentation rates have been low (e.g. Kiørboe *et al.,* 1994) and close to the maximum growth rate of the dominating *Thalassioisira mendiolana* observed during the exponential growth phase in our culture ($\sim$0.6 d^{-1}, Fig. 14). It may be worth noting that even though sedimentation constituted a relatively small fraction of the biomass it represents 25% of the growth production. The estimated grazing loss, up to about (0.1/0.4=) 25% of the production, is high relative to what can be found in other shallow water spring bloom systems (e.g. Kiørboe and Nielsen, 1994), but is consistent with the relatively dense populations of zooplankton occurring, 2–6 copepods l^{-1}.

The lack of a numerical response in zooplankton abundance and fecal pellet concentration to the increasing phytoplankton abundance is consistent with the much longer generation times of mesozooplankton compared to that of their phytoplankton prey. Thus, mesozooplankton is unable to control phytoplankton dynamics in a density dependent manner.

d. Larvacean house sedimentation

The good correlation between aggregate volume flux and sinking of intact phytoplankton cells suggests that sinking of aggregates was the major mechanism accounting for the vertical flux of phytoplankton cells during the study period. However, these aggregates were not formed by coagulation, but consisted of abandoned larvacean houses to which phytoplankton cells were attached. Particles primarily became attached through the filtering activities of the larvaceans when the houses were inhabited, whereas passive scavenging of particles by discarded houses was negligible (Hansen *et al.,* 1996). Larvaceans, in contrast to most other mesozooplankters, have population growth rates that are close to those of the phytoplankton (Hopcroft and Roff, 1995; Uye and Ichino, 1995). Yet there seemed to be no numerical response in larvacean abundance to the increasing diatom concentration, as judged from the temporal variation in the vertical flux of their abandoned houses (Fig. 11) and from their almost constant concentration in the upper 20 m of the water column (Fig. 6A). Larvaceans feed primarily on bacteria and small flagellates, while the larger diatoms are screened on their outer filter and not consumed (Alldredge, 1977). Consequently, their population sizes vary independently of diatom concentration. Thus, sinking of diatoms attached to larvacean houses, although occasionally much more important than in the case described here (Hansen *et al.,* 1996), does not exercise density-dependent population control on the diatoms.

e. Conclusions

Settling of phytoplankton and phytodetritus may occur by various mechanisms. This case study has identified and quantified the relative significance of the various mechanisms. Of the approximately 10% d^{-1} of the phytoplankton biomass (or 25% of the growth production) settling to the sea floor during this study about 30–50% was due to settling of fecal pellets, while the remaining sedimentation was due to settling of intact cells attached to larvacean houses. While phytoplankton aggregation and coagulation have been shown to be important in several diatom bloom systems for the sedimentation of intact cells (Alldredge and Gotschalk, 1989; Riebesell, 1991; Olesen, 1993; Kiørboe *et al.,* 1994; Alldredge *et al.,* 1995) it was unimportant in the system studied here. Also, settling of individual cells, suggested as significant in other studies (Waite *et al.,* 1992a; Pitcher, 1986), could account for only a small fraction of observed cell sedimentation in East Sound. Settling of cells collected on abandoned larvacean houses appeared to be the main mechanism for sinking of phytoplankton cells in East Sound during this study.

While coagulation implies density-dependent cell losses, neither grazing nor any of the settling mechanisms identified as important in this system worked in a density-dependent manner. Although all limiting the development of the phytoplankton populations, none of the mechanisms contributed to population regulation. Without coagulation, only about 10% of the standing stock of POC and phytoplankton sedimented per day, even in the presence of abundant copepod grazers and large particle generating larvaceans. This suggests that in the absence of significant coagulation rates, rapid mass sedimentation of

this algal bloom may be unlikely. Eventually, nutrient depletion or self shading may slow phytoplankton growth in this system, and thus control the bloom.

REFERENCES

Alldredge, A. L. 1977. House morphology and mechanisms of feeding in the Oikopleuri dae (Tunicata, Appendicularia). J. Zool, London, *181*, 175–188.

—— 1992. *In situ* collection and laboratory analysis of marine snow and large fecal pellets, *in* Marine particles: Analysis and Characterization, D. C. Hurd and D. W. Spencer, eds., Geophysical Monograph 63, American Geophysical Union, Washington, D.C., 43–46.

Alldredge, A. L. and C. C. Gotschalk. 1989. Direct observations of the mass flocculation of diatom blooms: characteristics, settling velocities and formation of diatom aggregates. Deep-Sea Res., *36*, 159–171.

Alldredge, A. L., C. Gotschalk, U. Passow and U. Riebesell. 1995. Mass aggregation of diatom blooms: Insights from a mesocosm study. Deep-Sea Res., *42*, 9–27.

Alldredge, A. L. and M. W. Silver. 1988. Characteristics, dynamics and significance of marine snow. Prog. Oceanogr., *20*, 41–82.

Anon. 1988. Baltic Marine Environmental Protection Commission—Helsinki Commission 1988. Guidelines for the Baltic Monitoring Programme for the third stage; Part D. Biological determinants. Baltic Sea Environmental Proceedings No. 27 D, 166 pp.

Beers, J. R., J. D. Trent, F. H. M. Reid and A. L. Shanks. 1986. Macroaggregates and their phytoplankton composition in the southern California Bight. J. Plankton Res., *8*, 475–487.

Betzer, P. R., W. J. Showers, E. A. Laws, C. D. Winn, G. R. DiTullio and P. M. Kroopuich. 1984. Primary productivity and particle fluxes on a transect of the equator at 153W in the Pacific Ocean. Deep-Sea Res., *31*, 1–11.

Bienfang, P. V. 1981a. Sinking rates of heterogeneous temperate phytoplankton populations. J. Plank. Res., *3*, 235–253.

—— 1981b. SETCOL—A technologically simple and reliable method for measuring phytoplankton sinking rates. Can. J. Fish. Aquat. Sci., *38*, 1289–1294.

Bodungen, von B., K. V. Brockel, V. Smetacek and B. Zeitschel. 1981. Growth and sedimentation of the phytoplankton spring bloom in the Bornholm Sea (Baltic Sea). Kieler Meeresforsch. Sonderh., *5*, 49–60.

Burd, A. and G. A. Jackson. 1996. The evolution of particle size spectra. I: Pulsed input. J. Geophys. Res., (submitted).

Butler, M. and H. G. Dam. 1994. Production rates and characteristics of fecal pellets of the copepod *Acartia tonsa* under simulated phytoplankton bloom conditions: implications for vertical fluxes. Mar. Ecol. Prog. Ser., *114*, 81–91.

Conover, R. C. 1978. Transformation of organic matter, *in* Marine Ecology, O. Kinne, ed., *4*, 221–499.

Crocker, K. M. and U. Passow. 1995. Differential aggregation of diatoms. Mar. Ecol. Prog. Ser., *117*, 249–257.

Dam, H. G. and D. Drapeau. 1995. Coagulation efficiency, organic-matter glues, and the dynamics of particles during a phytoplankton bloom in a mesocosm study. Deep-Sea Res. II., *42,* 111–123.

Drapeau, D. T., H. G. Dam and G. Grenier. 1994. An improved flocculator design for use in particle aggregation experiments. Limnol. Oceanogr., *39,* 723–729.

Farley, K. J. and F. M. M. Morel. 1986. Role of coagulation in the kinetics of sedimentation. Env. Sci. Tech., *20,* 187–195.

Hansen, J. L. S., T. Kiørboe and A. Alldredge. 1996. Marine snow derived from abandoned larvacean houses: sinking rates, particle content and mechanisms of aggregate formation. Mar. Ecol. Prog. Ser., *141,* 205–215.

Hansen, P. J. 1989. The red tide dinoflagellate *Alexandrium tamerensis:* Effects on behavior and growth of tintinnid ciliates. Mar. Ecol. Prog. Ser., *53,* 105–116.

Heath, M. R., K. Richardson and T. Kiørboe. 1990. Optical assessment of phytoplankton nutrient depletion. J. Plank. Res., *12,* 381–396.

Hopcroft, R. R. and J. C. Roff. 1995. Zooplankton growth rates: extraordinary production by the larvacean *Oikopleura dioica* in tropical waters. J. Plank. Res., *17,* 205–220.

Jackson, G. A. 1990. A model of the formation of marine algal flocks by physical coagulation processes. Deep-Sea Res., *37,* 1197–1121.

—— 1995a. Comparing observed changes in particle size spectra with those predicted using coagulation theory. Deep-Sea Res. II, *42,* 159–184.

—— 1995b. TEP and coagulation during a mesocosm experiment. Deep-Sea Res. II, *42,* 215–222.

Jackson, G. A., B. E. Logan, A. L. Alldredge and H. G. Dam. 1995. Combining particle size spectra from a mesocosm experiment measured using photographic and aperture impedance (Coulter and Elzone) techniques. Deep-Sea Res. II, *42,* 139–157.

Johnson, K. S., R. L. Petty and J. Thomsen. 1985. Flow injection analysis of seawater micronutrients. Adv. Chem. Ser., *209,* 7–30.

Jumars, P. A., D. L. Penry, J. A. Baross, M. J. Perry and B. W. Frost. 1989. Closing the microbial loop: dissolved carbon pathway to heterotrophic bacteria from incomplete ingestion, digestion and absorption in animals. Deep-Sea Res., *36,* 483–495.

Kiørboe, T. 1993. Turbulence, phytoplankton cell size, and the structure of pelagic food webs. Adv. Mar. Biol., *29,* 1–72.

Kiørboe, T., K. P. Andersen and H. G. Dam. 1990. Coagulation efficiency and aggregate formation in marine phytoplankton. Mar. Biol., *107,* 235–245.

Kiørboe, T. and J. L. S. Hansen. 1993. Phytoplankton aggregate formation: observations of patterns and mechanisms of cell sticking and the significance of exopolymeric material. J. Plank. Res., *15,* 993–1018.

Kiørboe, T., C. Lundsgaard, M. Olesen and J. L. S. Hansen. 1994. Aggregation and sedimentation processes during a spring phytoplankton bloom: A field experiment to test coagulation theory. J. Mar. Res., *52,* 297–323.

Kiørboe, T., F. Møhlenberg and K. Hamburger. 1985. Bioenergetics of the copepod *Acartia tonsa:* relation between feeding, egg production and respiration, and composition of specific dynamic action. Mar. Ecol. Prog. Ser., *26,* 85–97.

Kiørboe, T. and T. G. Nielsen. 1994. Regulation of zooplankton biomass and production in a temperate, coastal ecosystem. 1. Copepods. Limnol. Oceanogr., *39,* 493–507.

Kranck, K. and T. G. Milligan. 1988. Macroflocs from diatoms: *in situ* photography of particles in Bedford Basin, Nova Scotia. Mar. Ecol. Prog. Ser., *44,* 183–189.

Legendre, L. 1990. The significance of microalgal blooms for fisheries and for the export of particulate organic carbon in the oceans. J. Plank. Res., *12,* 681–699.

Journal of Marine Research [54, 6

Logan, B. E., U. Passow, A. L. Alldredge, H.-P. Grossart and M. Simon. 1995. Rapid formation and sedimentation of large aggregates is predictable from coagulation rates (half-lives) of transparent exopolymer particles (TEP). Deep-Sea Res. II, *42*, 203–214.

Lundsgaard, C. 1996. Use of high viscosity medium in studies of aggregates, *in* Sediment Trap Studies in Nordic Countries Three, S. Floderus, A.-S. Heiskanen, M. Olesen and P. Wassmann, eds., NurmitPrint Oy, Nurmijärvi, 141–152.

Mellor, G. L. and T. Yamada. 1982. Development of a turbulence closure model for geophysical fluid problems. Rev. Geophys. Space Phys., *20*, 851–875.

Noji, T. T., K. W. Estep, F. MacIntyre and F. Norrbin. 1991. Image analysis of faecal material grazed upon by three species of copepods: Evidence for coprohexy, coprophagy and coprochaly. J. Mar. Biol. Assoc. U.K., *71*, 465–480.

Olesen, M. 1993. The fate of an early diatom bloom in the Kattegat. Ophelia, *37*, 51–66.

Passow, U. 1991. Species-specific sedimentation and sinking velocities of diatoms. Mar. Biol., *108*, 449–455.

Passow, U. and A. L. Alldredge. 1995a. Aggregation of a diatom bloom in a mesocosm: The role of TEP. Deep-Sea Res. II, *42*, 99–109.

—— 1995b. A dye-binding assay for the spectrophotometric measurement of transparent exopolymer particles (TEP). Limnol. Oceanogr., *40*, 1326–1335.

Passow, U., A. L. Alldredge and B. E. Logan. 1994. The role of particulate carbohydrate exudates in the flocculation of diatom blooms. Deep-Sea Res. II, *41*, 335–357.

Pitcher, G. C. 1986. Sedimentary flux and the formation of resting spores of selected *Chaetoceros* species at two sites in the southern Benguela. S. Afr. J. Mar. Sci., *4*, 231–244.

Riebesell, U. 1991. Particle aggregation during a diatom bloom. II. Biological aspects. Mar. Ecol. Prog. Ser., *69*, 281–291.

Sharp, J. H. 1992. Total mass and particulate carbon, nitrogen, and phosphorus, *in* Marine Particles: Analysis and Characterization, D. C. Hurd and D. W. Spencer, eds., Geophysical Monograph 63, American Geophysical Union, Washington, D.C., 87–91.

Sharples, J. and P. Tett. 1994. Modelling the effect of physical variability on the midwater chlorophyll maximum. J. Mar. Res., *52*, 219–238.

Smetacek, V. 1980. Zooplankton standing stock, copepod fecal pellets and particulate detritus in Kiel Bight. Estuar. Coast. Mar. Sci., *11*, 477–490.

Strathmann, R. R. 1967. Estimating the organic carbon content of phytoplankton from cell volume or plasma volume. Limnol. Oceanogr., *12*, 411–418.

Strickland, J. D. and T. R. Parsons. 1968. A practical handbook of seawater analysis. Bull. Fish. Res. Bd. Can., *167*, 1–311.

Uye, S.-I. and S. Ichino. 1995. Seasonal variations in abundance, size composition, biomass and production rate of *Oikopleura dioica* (Fol) (tunicata, appendicularia) in a temperate eutrophic inlet. J. Exp. Mar. Biol. Ecol., *189*, 1–11.

Waite, A., P. K. Bienfang and P. J. Harrison. 1992a. Spring bloom sedimentation in a sub-arctic ecosystem. I: Nutrients and sinking. Mar. Biol., *114*, 119–129.

—— 1992b. Spring bloom sedimentation in a subarctic ecosystem. II: Succession and sedimentation. Mar. Biol., *114*, 131–138.

Wassmann, P. 1990. Relationships between primary production and export production in the boreal coastal zone of the North Atlantic. Limnol. Oceanogr., *35*, 464–471.